Performance Analysis of an LTE TDD Based Smart Grid Communications Network for Uplink Biased Traffic

Jason Brown and Jamil Y. Khan
School of Electrical Engineering and Computer Science,
The University of Newcastle, Callaghan, NSW 2308, AUSTRALIA
Email: {jbrown1, jamil.khan}@newcastle.edu.au

***Abstract*—LTE has been proposed as a possible wide area communications network for the Smart Grid. We analyze the performance of the LTE TDD mode when the uplink traffic (such as AMI meter readings and sensor data) is significantly higher than downlink traffic. We derive theoretical best case mean uplink latency figures for the relevant subset of LTE TDD uplink/downlink configurations (0, 1 and 6) and validate the findings using an OPNET simulation model. This leads to the conclusion that configuration 1 provides optimum uplink latency performance in general, but at high uplink traffic levels, only configuration 0 can reliably be used.**

***Index Terms*—LTE, TDD, Smart Grid Communications, Latency, Channel Utilization.**

I. INTRODUCTION

The Smart Grid ecosystem embraces a variety of applications such as Advanced Metering Infrastructure (AMI) and Demand Response (DR) [1]. Different realizations may lead to very different traffic patterns on the associated communication network depending upon the application mix deployed, the design of those applications and their configuration. In the short term, some of the applications most likely to be deployed are AMI meter reading transfer [2] and applications which involve monitoring of the Smart Grid infrastructure such as a Wide Area Measurement System (WAMS) [3]. These applications naturally involve more uplink than downlink data, therefore there is a reasonable likelihood that the overall traffic carried by the Smart Grid communications network will be uplink biased.

Long Term Evolution (LTE) [4] has been proposed as a possible wide area communications network for the Smart Grid [1][5] owing to its economies of scale and high spectral efficiency (and therefore low cost), support for a wide variety of frequency bands and bandwidths, support for multiple Quality-of-Service (QoS) classes, built in security and a flat all IP based architecture. LTE supports two duplexing modes: Frequency Division Duplex (FDD), in which the uplink and downlink are separated in frequency and both can be active at the same time, and Time Division Duplex (TDD), in which the uplink and downlink share the same frequency band and are separated in time such that simultaneous uplink/downlink operation is not possible [6]. Some of the advantages of TDD relative to FDD are lower cost of equipment due to the absence of a duplex filter, lower cost of spectrum because unpaired frequency allocations are not as attractive to large telecommunications carriers and the fact that the split of the total resources dedicated to the uplink and downlink can be easily optimized by varying the amount of time slots assigned to each. In fact, LTE TDD supports seven different such uplink/downlink allocation configurations with indexes 0-6 [7] which we discuss in a later section. The ability to match the LTE TDD uplink/downlink split of resources to a possible uplink biased Smart Grid traffic profile is the main focus of this paper. We examine the performance of the relevant LTE TDD configurations in carrying such traffic, in particular with respect to latency.

Only a small amount of research has been conducted into the performance of an LTE system in a Smart Grid environment. In [8], a Smart Grid based 20MHz LTE TDD system is simulated and uplink error rate curves are presented, but there is no treatment of latency. In [9], the authors consider the performance of a 5MHz LTE TDD system using uplink/downlink allocation configuration 1 in serving a Smart Grid Distribution Automation (DA) application. It is demonstrated that the maximum uplink latency is 66ms (allowing for up to 3 packet re-transmissions). The best case and mean uplink latency, or the use of different LTE TDD configurations, is not addressed. In this paper, we examine mean uplink latency under unloaded and loaded conditions. We consider a 5MHz LTE TDD system with uplink/downlink allocation configurations 0, 1 and 6, which are the most appropriate configurations for transporting traffic with an uplink bias.

The remainder of this paper is organized as follows. Section II examines the application of LTE TDD to Smart Grid communications, first focusing on likely Smart Grid traffic patterns including the possibility of asymmetrical traffic with an uplink bias, then addressing the strengths and weaknesses of LTE TDD in carrying such traffic. In Section III, we derive best case mean uplink latency figures for LTE TDD uplink/downlink allocation configurations 0, 1 and 6. Section IV describes an OPNET simulation environment based upon 100 Smart Grid measurement devices sending traffic in an unsynchronized manner over an LTE TDD network for each of the uplink/downlink allocation configurations 0, 1 and 6.

978-1-4673-4941-3/12/$31.00 ©2012 IEEE

We use the simulation environment to validate the earlier theoretical findings. Finally Section V provides conclusions and areas for further research.

II. Application of LTE TDD To Smart Grid Communications

A. Smart Grid Traffic Patterns

A conventional LTE wide area cellular network serving consumer, enterprise and government customers is typically characterised by the following traffic patterns: a) a significant proportion of the traffic is VoIP with symmetrical uplink and downlink resource usage, b) overall data traffic is asymmetric with higher downlink resource usage due to applications such as web browsing and video streaming (this is generally true even when uplink intensive applications such as photo/video upload accounted for), and c) the overall uplink/downlink split of resource usage is relatively time invariant.

The Smart Grid leads to very different traffic patterns. Firstly, VoIP is not expected to be a major application in the Smart Grid, and there are few if any envisaged applications which are naturally symmetric in their uplink/downlink resource usage. Secondly, assuming the deployment of typical Smart Grid applications such as AMI [2] and monitoring applications (e.g. WAMS [3]) which involve principally uplink application layer flows, there is the possibility that overall uplink resource usage will be higher than overall downlink resource usage as measured at the MAC layer. It is difficult to quantify the degree of the imbalance because it depends heavily on the complete set of Smart Grid applications and control systems which are deployed, their design (e.g. in respect of whether peer-to-peer or client/server models are utilised) and their configuration (e.g. the periodicity of data transfer for periodic sources).

We also note that the uplink/downlink split of resource usage in a Smart Grid communications network is likely to be time variant to a greater extent than a conventional cellular network. For example, if we consider peak periods of electricity demand, the Smart Grid operator may need to shed loads to retain network stability or reconfigure the network via switching to introduce an ancillary power generation facility, which clearly involves increasing the relative amount of downlink traffic. Another example involves a cascading fault situation which causes multiple sensors to send alarms to a server in a short interval, thereby increasing the relative amount of uplink traffic. Furthermore, these temporal variations in the uplink/downlink split of resource usage may be quite localised in spatial terms. Therefore there is a need to be able to accommodate or adapt to these changes (whether planned or unplanned) both in time and space.

B. LTE TDD Characteristics

The 3GPP Release 8 LTE standard supports both FDD and TDD duplexing modes [6]. The TDD mode involves using a single unpaired frequency band for uplink and downlink, and switching in the time domain between uplink and downlink resources. One of the important advantages of TDD mode is that the relative allocation of uplink and downlink resources in the time domain can be skewed to match any arbitrary required traffic pattern.

LTE TDD includes seven different uplink/downlink allocation configurations [7] with a frame comprising ten sub-frames of 1ms duration as listed in Table I. The sub-frames marked 'D' correspond to downlink sub-frames, those marked 'U' correspond to uplink sub-frames and those marked 'S' correspond to special sub-frames that serve multiple purposes, one of which is to act as a guard period between downlink to uplink switches and another of which is to serve as a reduced capacity downlink sub-frame [7].

Table I: LTE TDD Uplink/Downlink Allocation Configurations

Configuration	D-to-U periodicity	Sub-frame number									
		0	**1**	**2**	**3**	**4**	**5**	**6**	**7**	**8**	**9**
0	5 ms	D	S	U	U	U	D	S	U	U	U
1	5 ms	D	S	U	U	D	D	S	U	U	D
2	5 ms	D	S	U	D	D	D	S	U	D	D
3	10 ms	D	S	U	U	U	D	D	D	D	D
4	10 ms	D	S	U	U	D	D	D	D	D	D
5	10 ms	D	S	U	D	D	D	D	D	D	D
6	5 ms	D	S	U	U	U	D	S	U	U	D

The different uplink/downlink allocation configurations facilitate different asymmetric and (near) symmetric traffic profiles. For example, configuration 0 represents a maximally biased uplink with 6 U sub-frames per frame. If more than 60% of the traffic is uplink, we are still constrained to a using a maximum of 6 U sub-frames per frame. On the other hand, configuration 5 represents a maximally biased downlink with just 1 U sub-frame per frame. This demonstrates how the LTE TDD standard was designed assuming that a downlink biased allocation is more likely than an uplink biased allocation. Configurations 1 and 6 represent near symmetric profiles.

The configuration also determines whether there are one or two downlink to uplink switches per frame, and therefore one or two S sub-frames respectively. The advantage of two D-to-U switches per frame with a periodicity of 5ms is reduced latency, but it can only be achieved with the additional overhead of a second S sub-frame.

It should be noted that the use of highly asymmetric configurations can lead to performance issues because any unicast LTE data transfer always requires both uplink and downlink resources. For example, assume we have highly asymmetric traffic with a downlink bias and therefore use configuration 5 which only contains one U sub-frame per frame. Although we have 8 'D' sub-frames on which to send data from the network to a device per frame, the device can only send a HARQ acknowledgement in the single 'U' sub-frame, possibly resulting in a significant delay. In addition, if the network has sent data to the same device on several 'D' sub-frames, multiple acknowledgements are required in the single 'U' sub-frame, possibly creating a resource utilization issue. The LTE designers have incorporated some techniques to mitigate these issues such as multiple acknowledgements bundling for downlink packet transfer [10], but still the potential for performance issues exists.

In order to prevent co-channel interference between uplink and downlink, all TDD cells in the network must be frame synchronized and must possess the same uplink/downlink

allocation configuration at any arbitrary time. It is possible to change the configuration across the whole network, but only as a scheduled operations activity on an infrequent basis i.e. there is no facility for the configuration to be updated dynamically and/or automatically based upon prevailing traffic patterns. This severely limits the ability of an LTE TDD system to adapt to temporal and spatial variations in the offered traffic, which is problematic because the traffic profile of a Smart Grid is likely to be time and spatially variant.

III. Theoretical Analysis

In this section, we analyze the uplink latency of an LTE TDD system for uplink/downlink allocation configurations 0, 1 and 6. With reference to Table I, these are likely to be the only configurations that are of interest when the input traffic is asymmetrical with an uplink bias.

The latency of an uplink packet depends upon many factors including system load and channel conditions. For a TDD system, unlike an FDD system, it also depends upon the packet arrival timing relative to the frame timing. For example, consider uplink/downlink allocation configuration 1 in Table I. If an uplink packet enters the transmit buffer of a device during sub-frame 4, the device must wait until sub-frame 7 (i.e. the next U sub-frame) before signaling to the LTE network that it has a packet to send. On the other hand, if the packet arrives during sub-frame 6, the next U sub-frame is also sub-frame 7, so this second packet can in principle be transferred with lower latency.

Table II illustrates the best case theoretical latency of an uplink packet transmission as a function of the sub-frame in which the packet enters the transmit buffer of the device for configurations 0, 1 and 6. The assumptions underlying the calculations, including a lightly loaded system, are stated at the end of this section. A mean latency figure is also provided which assumes the packet arrival is equally likely to occur during any arbitrary sub-frame.

Table II: Best Case Uplink Latency Figures (SF = Sub-frame)

Sub-frame of packet	Latency (sub-frames or ms)		
	Config 0	Config 1	Config 6
0	9	8	12
1	8	7	11
2	7	6	10
3	6	10	9
4	10	9	10
5	9	8	9
6	8	7	8
7	7	6	7
8	6	10	14
9	10	9	13
Mean	**8**	**8**	**10.3**

A general heuristic method for calculating the best case uplink latency is as follows. First the device sends a Scheduling Request (SR) [11] on the PUCCH of the first U sub-frame following the sub-frame in which the packet enters its transmit buffer. The eNodeB replies with an uplink grant for the device on the PDCCH in the next instance of a D sub-frame. The uplink grant applies to the next instance of a U sub-frame, subject to the constraint that it must be at least 4 sub-frames later than the D sub-frame on which the uplink grant was received. The device sends its data packet on the PUSCH of this U sub-frame instance. The best case uplink latency is then the number of sub-frames from the time the packet entered the device transmit buffer to the sub-frame in which the packet was transmitted to the eNodeB. This procedure is illustrated in Fig. 1 for the case of uplink/downlink allocation configuration 1 with the packet entering the device transmit buffer in sub-frame 3.

However, this heuristic procedure does not accommodate all cases as the actual U sub-frame on which the device transmits the packet on the PUSCH is precisely specified via a look up table in [10]. An extract of this look up table is provided in Table III for the relevant configurations. For example, for configuration 0, if an uplink grant is received in sub-frame 0, this look up table indicates that the device should send its packet on the U sub-frame which is 4 sub-frames in the future. Some of the latency figures in Table II for the case of configuration 6 can only be derived accurately using the look up table. An example is illustrated in Fig. 2 with the packet entering the device transmit buffer in sub-frame 4.

Table III: Look Up Table Extract

Configuration	Sub-frame number									
	0	**1**	**2**	**3**	**4**	**5**	**6**	**7**	**8**	**9**
0	4	6				4	6			
1		6			4		6			4
6	7	7				7	7			5

There is an additional consideration for configuration 0 on account of the fact that there are only 4 D/S sub-frames on which the eNodeB may grant uplink transmissions across 6 U sub-frames. In order to facilitate load sharing on the 6 U sub-frames, the eNodeB can selectively override the lookup table allocations of 4 and 6 sub-frames given in Table III with a 7 sub-frame delay [7]. This clearly increases the mean delay for configuration 0, although it is difficult to quantify the effect as this feature is activated on demand by the eNodeB.

We note from Table II that configuration 6 has significantly higher best case mean uplink latency than configurations 0 and 1. This is somewhat surprising from first inspection as configuration 6 has more U frames than configuration 1, but the result is due to the precise sequence of D, S and U frames in the various configurations.

A device is not always allowed to send an SR in the first U sub-frame following the sub-frame in which the packet enters its transmit buffer. In fact, each device is assigned a specific offset within an SR period such that it must wait for its specific offset sub-frame to send its SR. The SR period can be one of 5, 10, 20, 40 or 80ms [7]. The implication of this is that the true best case mean latency is achieved by adding the mean latency figures in Table II to the mean SR delay. For example, for an SR period of 10ms, SR offsets are within the range 0-9ms with a mean value of 4.5ms. Therefore the adjusted best case mean latency figures for this example would be 12.5ms, 12.5ms and 14.8ms for uplink/downlink allocation configurations 0, 1 and 6 respectively.

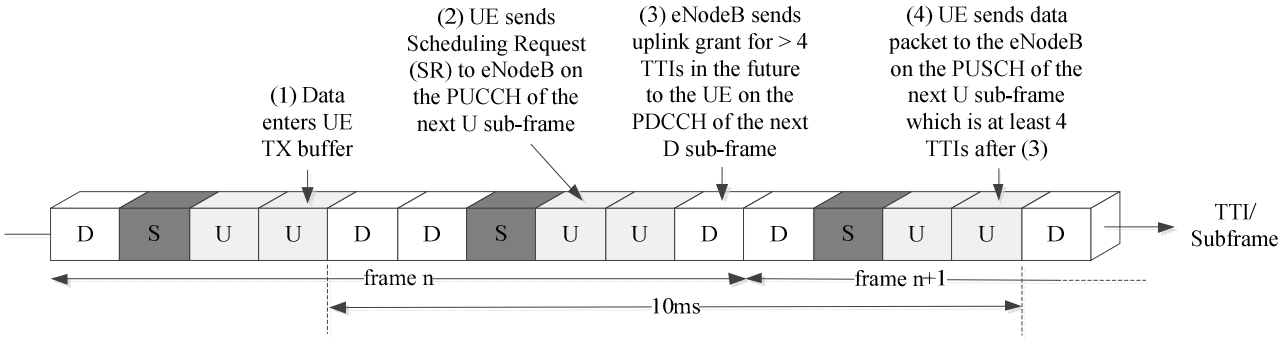

Fig. 1: Heuristic Best Case Uplink Latency Calculation for Uplink/Downlink Allocation Configuration 1 (packet enters the device transmit buffer in sub-frame 3)

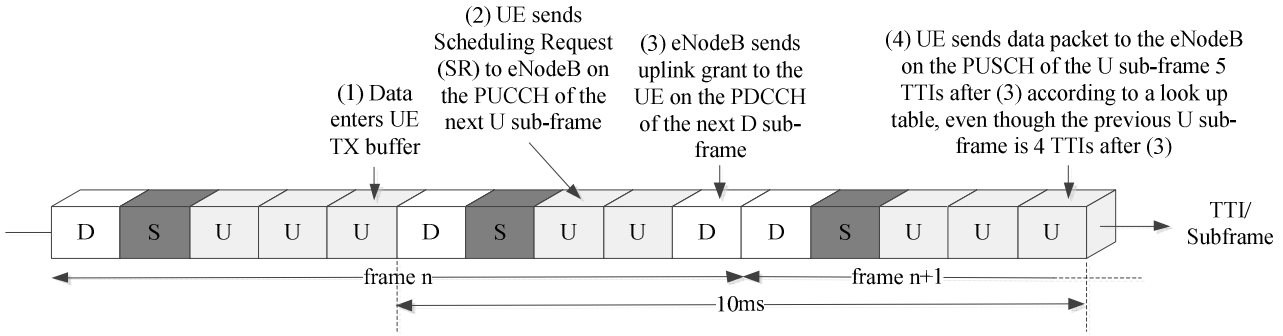

Fig. 2: Best Case Uplink Latency Calculation for Uplink/Downlink Allocation Configuration 6 (packet enters the device transmit buffer in sub-frame 4)

Finally, we list the assumptions that these best case uplink latency calculations involve: 1) The device must be in the RRC_CONNECTED state (as opposed to the RRC_IDLE state) [12] when the data packet arrives in the transmit buffer. If this is not the case, the device must first transition from the RRC_IDLE state to the RRC_CONNECTED state with a typical associated delay of 50-100ms. 2) The uplink data packet is sufficiently small that it can be transmitted in 1 U sub-frame. If this is not the case, there is an additional (fragmentation) delay. 3) If a D sub-frame immediately follows the U sub-frame on which an SR is received, the eNodeB is capable of returning an uplink grant in that following D sub-frame. Otherwise there is an additional delay due to SR processing at the eNodeB. 4) The system is lightly loaded so that the eNodeB can schedule an uplink grant for the device on the first available D sub-frame. Otherwise there is an additional scheduling delay at the eNodeB. 5) The eNodeB can successfully decode the initial uplink data packet transmission so that there is no need for a re-transmission which would incur additional delay.

IV. Simulation

A. OPNET Simulation Environment

In order to validate the theoretical best case uplink latency figures developed in Section III for LTE TDD uplink/downlink allocation configurations 0, 1 and 6, a simulation has been performed using the OPNET Modeler tool. The simulation model comprises an array of 100 Smart Grid sensors in an LTE TDD 5MHz cell, each of which is sending 32 byte payloads in an unsynchronised manner with inter-arrival times distributed according to an exponential distribution. The sensors might correspond to any Smart Grid measurement/monitoring function e.g. transformer temperature measurement, line tension etc. The mean data burst rate (i.e. the packet generation rate) was increased from 5pps (packets per second) to 60pps in intervals of 5pps to understand the impact of system loading on the uplink latency performance. Table IV lists the main parameters employed for the simulations.

Fig. 3 illustrates the sensor packet structure which comprises measurement/monitoring application data sent over UDP/IP.

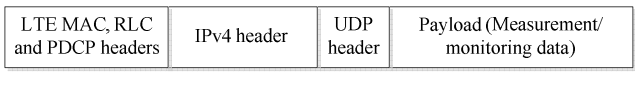

Fig. 3: Sensor Packet Structure When Transported over the LTE Air Interface

B. Latency

Fig. 4 illustrates the mean uplink end-to-end latency as a function of mean data burst arrival rate for the 100 sensors included in the simulation. It can be seen that the best case mean uplink latencies (i.e. for a data transmission frequency of 5pps) are 13.6ms, 12.4ms and 17.8ms for uplink/downlink allocation configurations 0, 1 and 6 respectively. This

compares to the predicted best case values in Section III of 12.5ms, 12.5ms and 14.8ms for a Scheduling Request (SR) period of 10ms. The fact that the simulated best case mean uplink latency for configuration 1 is slightly lower than the predicted value is due to the fact that the assigned SR offsets for different devices cannot be distributed in a precise uniform manner over the SR period. Note also that the simulation takes into account the effect of packet re-transmissions which occur when the eNodeB cannot successfully decode the original packet transmissions due to adverse channel conditions; these re-transmissions cause additional delay.

Table IV: Simulation Parameters

Parameter	***Value***
Frequency	3GPP Band 37 [13] (1920MHz uplink/downlink)
Channel bandwidth	5MHz (unpaired)
Duplexing scheme	Time Division Duplex (TDD)
Uplink/downlink allocation configuration	0 (6 U sub-frames) 1 (4 U sub-frames) 6 (5 U sub-frames)
Number of downlink symbols in S sub-frames	8
Cyclic prefix type	Normal
Maximum device Tx power	1W
Maximum eNodeB Tx power	40W
Device Rx sensitivity	-110dBm
eNodeB Rx sensitivity	-123dBm
Device height	1.5m
eNodeB height	40m
SR periodicity	10ms
Number of PUCCH channels	4
Channel models	Suburban fixed Erceg model with Terrain Type C [14] and a shadow fading standard deviation of 8.2dB.
Radio access network model	Single cell, 5km radius (78.5km^2)
Uplink traffic model	100 geographically fixed and non-synchronised sensors randomly placed in the cell sending UDP/IP packets with a 32 byte payload. The inter-arrival times of packets have an exponential distribution with a mean rate between 5pps and 60pps.
QoS for uplink traffic	Best effort on default bearer
Uplink scheduler algorithm	Dynamic fairness

It is clear from Fig. 4 that configuration 1 has the lowest uplink latency despite having the least (4) U sub-frames per frame of the three configurations. The fact that configuration 0 has slightly higher latency than configuration 1 is expected given the on demand override mechanism which uniquely applies to configuration 0 and which allows the eNodeB to load balance U frames at the expense of increased latency. Configuration 6 has the highest uplink latency. These observations agree with the theoretical analysis in Section III.

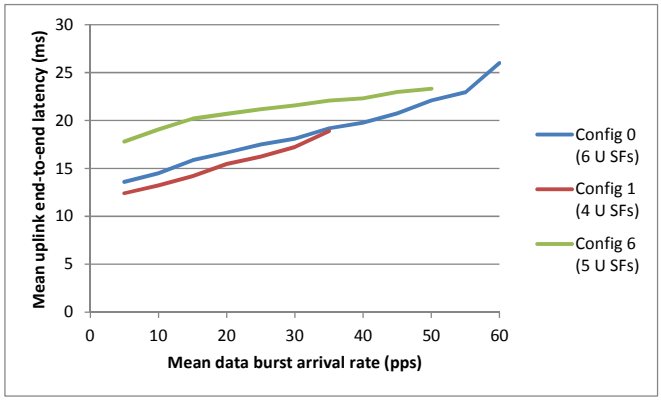

Fig. 4: Mean Uplink Latency

As the mean data burst arrival rate increases from 5pps (corresponding to a mean LTE uplink rate of 2.4Kbps per sensor) to 60pps (corresponding to a mean LTE uplink rate of 28.8Kbps per sensor), the mean uplink latency increases in an approximately linear manner. Eventually all available U sub-frames are consumed by the increasing traffic load and no more traffic can be serviced per unit time. At this point, the line for a particular graph terminates. This occurs with a relatively low load for configuration 1 because this configuration has the least U sub-frames per frame and at a relatively high load for configuration 0 because this configuration has the most U sub-frames per frame.

Fig. 5 illustrates the mean uplink end-to-end latency as a function of mean (uplink) data burst arrival rate for various uplink/downlink traffic splits. The downlink packets have the same payload size of 32 bytes as the uplink packets, but are sent less frequently (at ¼ the mean rate for the 20% downlink traffic scenario and at ½ the mean rate for the 33% downlink traffic scenario). It can be seen that the mean uplink latency increases as the volume of downlink traffic increases. This is primarily due to congestion on the PDCCH channel which the eNodeB uses both to make downlink assignments and to allocate uplink grants to users.

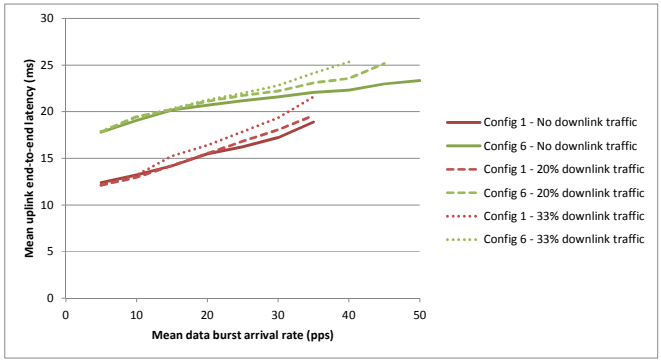

Fig. 5: Mean Uplink Latency for Various Traffic Splits

C. Channel Utilization

Fig. 6 and Fig. 7 illustrate the mean PDCCH channel utilization and mean PUSCH channel utilization respectively as a function of mean data burst arrival rate for the 100

sensors included in the simulation. In the case of the PDCCH, the mean utilization is in respect of the percentage of occupied Control Channel Elements (CCEs) which the eNodeB uses to assign uplink grants to the devices, whereas in the case of the PUSCH, the mean utilization is in respect of the percentage of occupied uplink Resource Block (RB) pairs that carry data packets. The utilization figures do not represent how efficiently each CCE or uplink RB pair is being utilized, only whether they are being utilized or not.

Configuration 0 has the highest number (6) of U sub-frames and lowest number (4) of D/S sub-frames of all the configurations, therefore it is not surprising that it has the lowest PUSCH channel utilization but the highest PDCCH channel utilization. Conversely, configuration 1 has the lowest number (4) of U sub-frames and highest number (6) of D/S sub-frames of all the configurations, therefore it is not surprising that it has the highest PUSCH channel utilization but the lowest PDCCH channel utilization.

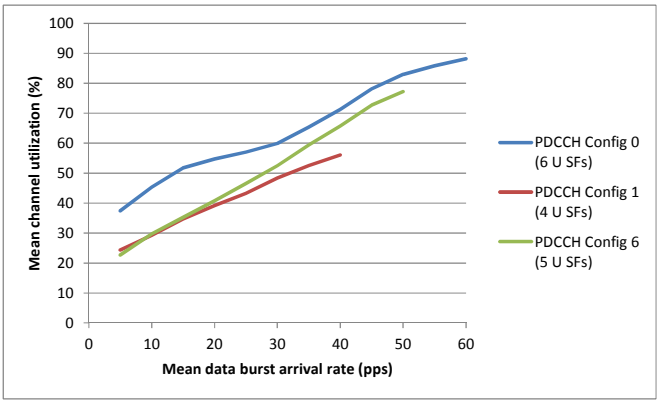

Fig. 6: Mean PDCCH Channel Utilization

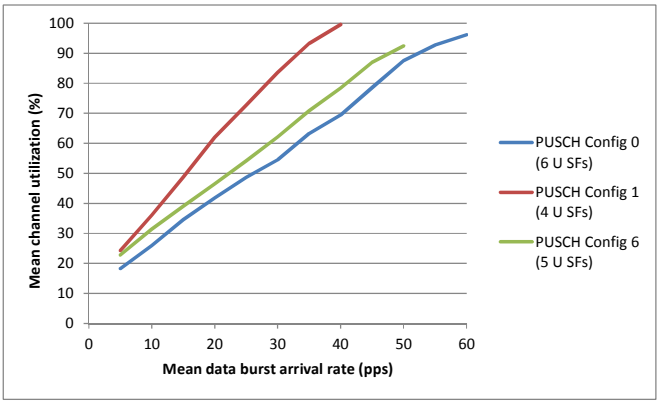

Fig. 7: Mean PUSCH Channel Utilization

V. CONCLUSIONS

In this paper, we have analyzed the performance of a standard Release 8 LTE TDD wide area communications system for use in a Smart Grid communications scenario with an uplink biased traffic profile. The LTE TDD uplink/downlink allocation profiles 0, 1 and 6, which are the most suitable for an uplink biased traffic profile, have been compared with respect to latency both from an analytical and a simulation perspective. We showed that configuration 1 has the lowest mean uplink latency even though it has the lowest number (4) of U sub-frames per frame. Configuration 6 has the highest mean uplink latency and is therefore less suitable for a Smart Grid communications network supporting delay sensitive applications.

We conclude that configuration 1 is preferred from a latency perspective for uplink biased traffic, but as the uplink traffic load increases, it becomes saturated before configuration 0 because the latter possesses more U sub-frames per frame. Ideally we would switch the configuration in real time from configuration 1 to configuration 0 as the uplink traffic surpasses a certain threshold, but LTE TDD does not currently support dynamic switching of the uplink/downlink allocation configuration. We note, however, that the area of dynamic TDD configuration switching is an active area of research [15].

Further work will focus on proposing new LTE TDD uplink/downlink allocation configurations for use in a Smart Grid environment (in particular to support more than 6 U sub-frames per frame for heavily uplink biased traffic).

ACKNOWLEDGEMENTS

This work has been supported by Ausgrid and the Australian Research Council (ARC).

REFERENCES

[1] Patel A., Aparicio J., Tas N., Loiacono M., Rosca J., “Assessing Communications Technology Options for Smart Grid Applications”, Smart Grid Communications (SmartGridComm), 2011 IEEE International Conference on, 2011, pp. 126-131

[2] Jun Wang and Victor C. M. Leung., “A survey of technical requirements and consumer application standards for IP-based smart grid AMI network”, Information Networking (ICOIN), 2011 International Conference on, 2011, pp. 114 – 119.

[3] Yingchen Zhang et al., “Wide-Area Frequency Monitoring Network (FNET) Architecture and Applications”, Smart Grid, IEEE Transactions on, Volume: 1, Issue: 2, September 2010, pp. 159 – 167.

[4] 3GPP TR 25.913 V8.0.0 (2008-12), “Requirements for Evolved UTRA (E-UTRA) and Evolved UTRAN (E-UTRAN)", Release 8

[5] Parikh, P.P.; Kanabar, M.G.; Sidhu, T.S., “Opportunities and challenges of wireless communication technologies for smart grid applications”, IEEE Power and Energy Society General Meeting, 2010.

[6] 3GPP TS 36.300 V8.12.0 (2010-03), “Evolved Universal Terrestrial Radio Access (E-UTRA) and Evolved Universal Terrestrial Radio Access Network (E-UTRAN); Overall description; Stage 2”, Release 8

[7] 3GPP TS 36.211 V8.9.0 (2009-12), “Evolved Universal Terrestrial Radio Access (E-UTRA); Physical Channels and Modulation", Release 8

[8] Zhao Feng, Liu Jianming, Hu Dan, Zhang Yuexia, “Study on the application of advanced broadband wireless mobile communication technology in smart grid”, Power System Technology (POWERCON), 2010 International Conference on, 2010.

[9] Peng Cheng, Li Wang, Bin Zhen, Shihua Wang, “Feasibility Study of Applying LTE to Smart Grid”, IEEE First International Workshop on Smart Grid Modeling and Simulation (SGMS) - IEEE SmartGridComm 2011

[10] 3GPP TS 36.213 V8.8.0 (2009-09), “Evolved Universal Terrestrial Radio Access (E-UTRA); Physical layer procedures”, Release 8

[11] 3GPP TS 36.321 V8.10.0 (2011-09), “Evolved Universal Terrestrial Radio Access (E-UTRA); Medium Access Control (MAC) protocol specification”, Release 8

[12] 3GPP TS 36.331 V8.15.0 (2011-09), “Evolved Universal Terrestrial Radio Access (E-UTRA); Radio Resource Control (RRC); Protocol specification”, Release 8.

[13] 3GPP TS 36.101 V8.16.0 (2011-12), “Evolved Universal Terrestrial Radio Access (E-UTRA); User Equipment (UE) radio transmission and reception", Release 8

[14] V. Erceg et al., “An empirically based path loss model for wireless channels in suburban environments”, IEEE JSAC, vol.17, no.7, July 1999, pp. 1205-1222.

[15] Mohammed Al-Rawi and Riku Jantti, “A Dynamic TDD Inter-Cell Interference Coordination Scheme for Long Term Evolution Networks”, PIMRC, IEEE 22nd International Symposium on, 2011.